Published in final edited form as:

Exp Neurol. 2017 January ; 287(Pt 2): 254–260. doi:10.1016/j.expneurol.2016.07.023.

Influence of developmental nicotine exposure on glutamatergic neurotransmission in rhythmically active hypoglossal motoneurons

Marina Cholanian[1], **Gregory L. Powell**[1], **Richard B. Levine**[1,2], and **Ralph F. Fregosi**[1,2,*]

[1]Department of Physiology, University of Arizona College of Medicine, Tucson, Arizona, USA 85724

[2]Department of Neuroscience, University of Arizona, Tucson, Arizona, USA 85724

Abstract

Developmental nicotine exposure (DNE) is associated with increased risk of cardiorespiratory, intellectual, and behavioral abnormalities in neonates, and is a risk factor for apnea of prematurity, altered arousal responses and Sudden Infant Death Syndrome. Alterations in nicotinic acetylcholine receptor signaling (nAChRs) after DNE lead to changes in excitatory neurotransmission in neural networks that control breathing, including a heightened excitatory response to AMPA microinjection into the hypoglossal motor nucleus. Here, we report on experiments designed to probe possible postsynaptic and presynaptic mechanisms that may underlie this plasticity. Pregnant dams were exposed to nicotine or saline via an osmotic mini-pump implanted on the 5th day of gestation. We used whole-cell patch clamp electrophysiology to record from hypoglossal motoneurons (XIIMNs) in thick medullary slices from neonatal rat pups (N= 26 control and 24 DNE cells). To enable the translation of our findings to breathing-related consequences of DNE, we only studied XIIMNs that were receiving rhythmic excitatory drive from the respiratory central pattern generator. Tetrodotoxin was used to isolate XIIMNs from presynaptic input, and their postsynaptic responses to bath application of L-glutamic acid (glutamate) and α-amino-3-hydroxy-5-methyl-4-isoxazolepropionic acid (AMPA) were studied under voltage clamp. DNE had no influence on inward current magnitude evoked by either glutamate or AMPA. However, in cells from DNE animals, bath application of AMPA was associated with a right shift in the amplitude distribution (P = 0.0004), but no change in the inter-event interval distribution of miniature excitatory postsynaptic currents (mEPSCs). DNE had no influence on mEPSC amplitude or frequency evoked by glutamate application, or under (unstimulated) baseline conditions. Thus, in the presence of AMPA, DNE is associated with a small but significant increase in quantal size, but no change in the probability of glutamate release.

*Correspondence to: Ralph F. Fregosi, PhD, Department of Physiology, University of Arizona, College of Medicine, 1501 N. Campbell Ave, Tucson, AZ, 85724, USA, fregosi@email.arizona.edu, Phone: (520) 621-2203.

DISCLOSURE STATEMENT: The authors have nothing to disclose.

Keywords

AMPA; breathing; glutamate; hypoglossal nucleus; nicotine; desensitization

Introduction

According to the Centers for Disease Control (CDC) cigarette smoking is one of the leading causes of preventable disease in the United States, resulting in 1 out of 5 deaths annually (www.cdc.gov/tobacco). Nicotine is the primary neurotoxin in tobacco products (Abreu-Villaca et al., 2003; Eriksson et al., 2001; Ginzel et al., 2007; Pauly and Slotkin, 2008), as it has been strongly associated with altered development of neurons throughout the brain (Eriksson, 1997; Slotkin, 2004), including brainstem neurons involved in the control of breathing (Dwyer et al., 2009; Hafstrom et al., 2005; Muhammad et al., 2012; Pilarski et al., 2011). Despite an overall decline in the use of cigarettes in the U.S. in the last decade, the incidence of nicotine use during gestation remains unaddressed, as nicotine replacement therapy (patch, gum) is commonly prescribed to pregnant women who continue to smoke (Oncken, 2012). Developmental nicotine exposure (DNE) in rodents is a widely accepted model for studying the effects of *in utero* exposure to nicotine (Slotkin, 2004). Chronic nicotine exposure causes widespread desensitization of nicotinic acetylcholine receptors (nAChRs), leading to increased receptor expression, but a reduction in synaptic efficacy (Gentry and Lukas, 2002; Marks et al., 1983; Marks et al., 1985). This paradox results in a "functional loss" of nAChRs and is due to long-term receptor desensitization. Consistent with this, our previous work (Pilarski et al., 2012) showed that DNE caused functional desensitization of nAChRs on hypoglossal motoneurons (XIIMNs). Hypoglossal motoneurons control the activity of the tongue muscles, which play an important role in swallowing and chewing, as well as breathing, especially during sleep (Eisele et al., 2003; Kezirian et al., 2010), and excitatory drive to XIIMNs relies importantly on glutamatergic neurotransmission (Revill et al., 2015; Steenland et al., 2006).

Our laboratory previously reported that DNE decreased excitatory synaptic input in XIIMNs of neonatal rats (Pilarski et al., 2011), and increased the response of XIIMNs to microinjection of glutamate or AMPA into the hypoglossal motor nucleus (Jaiswal et al., 2013). These observations lead to the development of a model that is based on the working hypothesis that the reduced presynaptic excitatory input leads to an increased density, and/or a functional change, in postsynaptic glutamate receptors, as summarized in Fig. 1. Here we focus on two components of this model, namely postsynaptic changes in glutamatergic transmission, and alterations in the quantity and frequency of glutamate release from glutamatergic neurons that synapse on XIIMNs.

We used the whole-cell patch-clamp technique to record from rhythmically-active XIIMNs in thick medullary slices. Postsynaptic effects were examined by bath applying glutamate or AMPA in the presence of tetrodotoxin (TTX) and recording the kinetics and magnitude of the evoked inward current. We also examined changes in quantal synaptic transmission by recording the frequency and amplitude of miniature excitatory postsynaptic currents (mEPSCs), under baseline conditions and also during bath application of glutamate or

AMPA. In the presence of AMPA, mEPSC amplitude was larger in DNE than in control and their frequency greater, consistent with an increase in quantal size and an increase in the probability of glutamate release; mechanisms that may explain these observations are addressed in the Discussion.

Materials and Methods

2.1. Animals

We used a total of 50 Sprague-Dawley rats of either sex, aged from postnatal day zero (P0) through postnatal day four (P4). This neonatal period corresponds to a gestational age of 29–34 weeks in humans (Ballanyi et al., 1999). The nicotine-exposed neonates were taken from 19 separate litters; the saline-exposed neonates from 15 different litters; and the unexposed from 3 litters. From each litter, 1–3 neonates were used. All neonates were born via spontaneous vaginal delivery from pregnant adult female rats purchased from Charles River Laboratories (Wilmington, MA). Neonatal rat pups were housed together with their mothers and siblings until they were studied. Dams were housed in the Animal Care Facility at the University of Arizona under a 12: 12 h light/dark cycle (lights on 07:00 h) with water and food available *ad libitum*, in a quiet room at 22°C and 20–30% relative humidity. All protocols were approved by the University of Arizona Institutional Care and Use Committee and conformed to National Institutes of Health guidelines.

2.2. Developmental nicotine exposure

DNE was achieved by subcutaneous implantation of Alzet 1007D mini-osmotic pumps (Alzet Corp., CA, USA) into pregnant dams on gestational day 5 under aseptic conditions, as previously described (Fregosi et al., 2004; Huang et al., 2004; Luo et al., 2007). The pumps allow for fluid infusion into subcutaneous space at a rate of 2.5 μL h^{-1} for 28 days. This infusion rate achieves mean nicotine bitartrate delivery of 6 mg kg^{-1} day^{-1} throughout gestation. We previously showed that this regimen produces plasma levels of cotinine, a major metabolite of nicotine with a long half-life (20–24 h), ranging from 60–92 ng/mL (Powell et al., 2015). This is comparable to average cotinine levels (88 ng/mL) found in the umbilical cord blood of newborns whose mothers smoked on average 95 cigarettes/week (Berlin et al., 2010).

2.3. Medullary slice preparation

Pups of either sex were removed from their home cages at random and weighed. Animals were anesthetized by hypothermia until unresponsive to a paw pinch, and decerebrated at the coronal suture. The vertebral column and ribcage were exposed, moved to a dissection dish filled with cold (4–8°C) oxygenated (95% O_2-5% CO_2) artificial cerebrospinal fluid (aCSF), composed of (in mM): 120 NaCl, 26 $NaHCO_3$, 30 glucose, 1 $MgSO_4$, 3 KCl, 1.25 NaH_2PO_4, and 1.2 $CaCl_2$ with pH adjusted to 7.4 and osmolarity adjusted to 300–325 mOsm. The spinal cord and brainstem were glued to an agar block with superglue, rostral surface up, for serial microsectioning in a vibratome (VT1000; Leica). Transverse medullary slices were taken in chilled oxygenated aCSF until the most rostral hypoglossal nerve (XIIn) rootlets were near the surface of the tissue. A single 700-μm slice was taken to capture the majority of hypoglossal motor nucleus and the preBotzinger complex, which can drive

rhythmic respiration-related bursting in the medullary slice. The slice was then transferred to fresh aCSF that was continuously oxygenated with 95%O_2-5%CO_2 and allowed to equilibrate at room temperature for 1–2 hours before recording. Slices were then transferred to the recording chamber and perfused with oxygenated aCSF. To evoke rhythmic bursting of XIIMNs, the KCl of the perfusate was raised to 9 mM. We used rhythmic slices because we are interested in motoneurons that play a role in breathing. High potassium is commonly used to evoke rhythmic bursting in brainstem slices, though we realize that some motoneurons that were rhythmic in high potassium may have not been rhythmic when exposed to physiological levels of extracellular potassium, though the rhythmic slice does mimic conditions of high respiratory drive.

2.4. Electrophysiology

XIIMNs were visualized with an Olympus BX-50WI fixed-stage microscope (X40 water-immersion objective, 0.75 N.A.) with infrared and differential contrast optics and a video camera (C25400-07, Hamamatsu). XIIMNs were approached with a glass pipette (4–8 MΩ) pulled from thick-walled borosilicate glass capillary tubes (OD: 1.5 mm, ID: 0.75 mm) and filled with intracellular solution which contained (in mM): 135 K-gluconate, 4 KCl, 10 HEPES, 5 ATP (Mg^{2+} salt), 0.375 GTP, and 12.5 phosphocreatine, with pH adjusted to 7.2 and osmolarity of 275–300 mOsm. The electrophysiology equipment consisted of Digidata 1440 and Multiclamp 700B amplifier (Molecular Devices).

2.5. Drugs

Most drugs were purchased from Sigma (St. Louis, MO, USA). Tetrodotoxin was purchased from R&D (Minneapolis, MN, USA). The drugs were mixed on the day of the experiment in modified aCSF (9 mM KCl) with the following concentrations: tetrodotoxin (TTX, 1 μM), αamino-3-hydroxy-5-methyl-4-isoxazolepropionic acid (AMPA, 2.5 μM), 6-cyano-7-nitroquinoxaline-2,3-dione (CNQX, 20 μM), and L-glutamic acid monosodium salt hydrate (glutamate, 200 μM). The drug solutions were oxygenated and were delivered to the recording chamber at a rate of 1.5–2 ml/min, with the temperature controlled at 27°C (TC-324B temperature controller, Warner Instrument Corporation). A summary of drug concentrations and durations of application is provided in Table 1.

2.6. Protocols

A total of 26 control and 24 DNE rhythmically active XIIMNs (1 cell from each animal) were studied under whole cell voltage-clamp (Vhold = −70 mV). The slow and fast components of the voltage transient were cancelled. The series resistance was compensated with the bandwidth set at 4 kHz and correction at 60%. A small voltage-step (from −70 to −75 mV) protocol was performed to calculate motoneuron input resistance. This was followed by 1-min recording in current-clamp mode (I hold = 0 pA, pipette offset adjusted) to check the stability of the cell and to measure the resting membrane potential. We then performed a square-pulse current-step protocol to determine the firing threshold. Current steps (800 msec duration) were initiated at 0 pA and ranged from −200 pA to +350 pA in 50pA increments. Then, the cell was switched back to voltage clamp mode (Vhold = −70 mV), the rhythmic activity was recorded for 1 min, and TTX was bath applied for 2 min to establish a new, stable baseline. These studies were then followed by bath application of

cocktails containing AMPA + TTX (N=13 control, 11 DNE) or glutamate + TTX (N=13 control, 13 DNE) for 5 min. This was followed by bath application of AMPA + TTX + CNQX, or glutamate + TTX + CNQX for 5 min, followed by a washout with TTX alone (Fig. 2). Importantly, the addition of CNQX always abolished the inward current and mEPSCs, confirming that both were mediated byAMPA receptors. At the end of each experiment, the small voltage-step protocol (from −70 mV to −75 mV) was repeated to measure the input resistance and confirm that the gigaohm seal was intact.

2.7. Data analysis and Statistics

Analysis of the voltage- and current-clamp data obtained in Clampex (Molecular Devices, Sunnyvale, CA) was performed in Clampfit (Molecular Devices, Sunnyvale, CA) and with custom scripts written in Spike2 (CED, Cambridge, UK). The analysis of miniature excitatory postsynaptic currents was done using MiniAnalysis 6.0.7 (Synaptosoft, Decatur, GA). The quantitative data were statistically analyzed using Prism (GraphPad Software, Inc., La Jolla, CA) and SPSS (IBM, Armonk, NY). Unpaired t-tests were used to compare treatment groups for the following variables: input resistance, resting membrane potential, weight, age, holding current, the peak and total (area under the curve) inward current produced with drug application, and the time needed to reach 1/2-peak amplitude. We also measured the inward current produced at 20, 40, 60, 80 and 100% of the total drug application time, and. analyzed these data with 2-way repeated measures ANOVA, with treatment (control, DNE) and the % drug application time the main factors.

Average mEPSC amplitude and frequency at baseline and during application of AMPA or glutamate were compared between the treatment groups using 2-way ANOVA. To examine changes in the entire population of mEPSCs under each condition (baseline, drug) and treatment (control, DNE), we constructed cumulative frequency distribution plots, and fit the data with a Gaussian distribution model using Prism software. We expressed the cumulative frequency as fractions ranging from 0–1, such that a value of 0.5 defines the midpoint of the normalized mEPSC amplitude or frequency distribution (see Fig. 6). Statistical comparisons were made by comparing the means and standard deviations of the non-linear, Gaussian distributions. For all analyses, data were considered statistically significant if $P \leq 0.05$. Data in all figures and tables are represented as Means ± SEM, unless stated otherwise.

Results

DNE does not alter AMPA- and glutamate-induced inward currents

At baseline, the frequency of rhythmic, respiration-related XIIMN bursts did not differ between the groups, although there was a trend for a higher frequency in the DNE group (Control, 14.3 ± 2.0, DNE, 18.0 ± 2.9, P = 0.293; Fig. 3). There were no significant differences in the age and weight of the animals, or the resting membrane potential or input resistance of rhythmically active XIIMNs in either the AMPA or glutamate studies (Fig. 4). The holding current needed to establish the voltage clamp at −70 mV was also the same in XIIMNs from control (175 ± 24 pA) and DNE animals (202 ± 35 pA).

The bath application of AMPA or glutamate (concomitantly with TTX in order to assess the direct effect of the agonist on the XIIMN) produced a large and rapid inward current (Fig. 2A–B). However, neither the peak nor total inward current magnitude differed in cells from control and DNE animals in response to bath application of either AMPA (peak inward current: control −490 ± 93 pA; DNE −569 ± 142 pA, P = 0.66: total inward current: control −138 ± 26 nA*s; DNE, −168 ± 37 nA*s, P = 0.52) or glutamate (peak inward current: control −193 ± 42; DNE −148 ± 43 pA, P = 0.45: total inward current: control −54 ± 11 nA*s; DNE, −42 ± 13 nA*s, P = 0.51).

We also measured the evoked inward current at 20, 40, 60, 80 and 100% of the drug application time, as shown in the upper panels of Fig. 5. The current evoked with AMPA increased with time (P < 0.0001), but neither treatment nor the time-by-treatment interaction was significant (P = 0.54 and 0.71, respectively). The current evoked by glutamate also increased with time (P < 0.0001), but there were no treatment (P = 0.5) or time-by-treatment interactions (P = 0.74). We also computed the time to reach half of the peak inward current ($T_{1/2}$) evoked by AMPA or glutamate, as shown in the two bottom panels of Fig. 5. There was a trend for a more rapid change in inward current in XIIMNs from DNE animals with both AMPA (control, 105 ± 18 s, DNE 69.7 ± 9.3, P = 0.089) and glutamate (control, 72.9 ± 13.2 s, DNE 45.3 ± 11.1, P = 0.12), but the differences were not significant in either case.

DNE alters mEPSC amplitude

The bath application of TTX blocks action potential dependent synaptic inputs onto XIIMNs, but the spontaneous release of neurotransmitter by presynaptic neurons remains intact and can be measured as mEPSCs from the postsynaptic cell (Vautrin and Barker, 2003). We analyzed the amplitude and frequency of mEPSCs under baseline conditions, and throughout the first minute of drug application. Under baseline conditions, we found no differences for average mEPSC amplitude or frequency, and no differences in the cumulative probability distributions in cells from control and DNE animals (data not shown). There were also no treatment effects for mEPSC amplitude or frequency in response to bath application of glutamate. In contrast, after bath application of AMPA (Fig. 6, top panel) the mEPSC amplitude distribution in XIIMNs from DNE animals was right-shifted as compared to control (P = 0.0004), indicating that the population of mEPSC amplitudes from DNE XIIMNs in the presence of AMPA is on average larger than those recorded from control XIIMNs. Average and SD values for the midpoint of the probability distribution were: control distribution, 20.4 ± 8.4, 163 degrees of freedom and $r^2 = 0.97$; corresponding values for the DNE probability distribution were 25.3 ± 9.7, 148 and 0.97. In contrast, after AMPA application the distribution of inter-event intervals was shifted slightly to the left in DNE as compared to control motoneurons, but the difference was not significant (P = 0.47) (Fig. 6, bottom panel).

Discussion

In the present study we sought to better understand changes in glutamatergic neurotransmission in XIIMNs from neonatal rats that were exposed to nicotine during development. We previously showed that DNE is associated with an exaggerated excitatory

response in XIIMNs when AMPA or glutamate was injected into the hypoglossal motor nucleus (Jaiswal et al., 2013), as well as a reduction in baseline glutamatergic excitatory synaptic input (Pilarski et al., 2011). Thus, DNE may be altering the postsynaptic response of XIIMNs to glutamate, the release of glutamate by presynaptic neurons or both. To test for a pure postsynaptic response to glutamate, we applied agonists in the presence of TTX and measured the magnitude of the evoked inward current. To examine possible changes in presynaptic parameters, we measured miniature EPSCs. We found that presynaptic and postsynaptic effects were mediated by AMPA receptors, as responses to both glutamate and AMPA were abolished by the AMPA receptor antagonist CNQX.

Postsynaptic mechanisms

We first tested the hypothesis that DNE caused a change in the postsynaptic sensitivity of XIIMNs to glutamate or AMPA. Such a change might be caused, for example, by a compensatory increase in the density of postsynaptic receptors, as schematized in Fig. 1. The bath application experiments reject this hypothesis in its most simple form, as the magnitude of post-synaptic inward currents in response to glutamate or AMPA in rhythmically active XIIMNs were not altered by DNE. Furthermore, although we saw a trend for a faster time to half-peak amplitude in cells from the DNE group (Fig. 5), a finding that could potentially suggest a change in the kinetics of receptors on the postsynaptic cell, this difference was not statistically significant.

Although mEPSC amplitudes and interevent interval distributions were not different at baseline, the amplitude of mEPSCs, which we observed after AMPA application was greater in DNE cells. This may also reflect a postsynaptic effect of DNE, such as an increase in the number and/or a change in the structure or function of postsynaptic glutamate receptors (Pinheiro and Mulle, 2008; Vautrin and Barker, 2003). However, our observation that bath application of drugs did not result in a larger or faster inward currents in XIIMNs does not support this mechanism. In addition, our earlier observations using immunocytochemistry revealed an overall reduction in the expression of glutamate receptors in the hypoglossal motor nucleus as a result of DNE (Jaiswal et al., 2013). Nevertheless, we cannot confidently exclude the possibility that DNE changed the postsynaptic sensitivity to glutamate to yield larger mEPSCs, as bath-applied agonists may obscure changes in postsynaptic sensitivity. Bath application allows compounds to diffuse freely and broadly within the slice affecting multiple neurotransmitter and neuromodulatory systems that may express presynaptic glutamate receptors, which when stimulated could evoke transmitter release (Funk and Greer, 2013). Furthermore, bath application activates all postsynaptic sites simultaneously. We have recently reported that DNE leads to a significant alteration of XIIMN dendritic branching (Powell et al., 2016). Therefore, there may be rearrangement of synaptic locations relative to the cell body, or changes in the subtypes or density of glutamatergic receptors at a subset of postsynaptic sites that lead to increased mEPSC amplitude but not increased overall response of the XIIMNs to bath application of agonists. Focal pressure ejection would have confined the drugs to a smaller region, but the inability to precisely replicate drug dose and time of action from cell-to-cell would have created more serious problems in the interpretation of the results.

Presynaptic mechanisms

As indicated above, AMPA application was associated with a right shift of the normalized mEPSC amplitude distribution in XIIMNs from DNE animals (Fig. 6), which suggests a presynaptic effect of DNE. That this was observed only in response to bath application of AMPA, and not under baseline conditions, suggests that the increased release, as suggested by larger mEPSCs, was mediated by AMPA receptors on presynaptic glutamatergic neurons ("autoreceptors"), as observed in other neuronal populations (Pinheiro and Mulle, 2008). Although a shift in the mEPSC amplitude distribution is often attributed to altered postsynaptic receptor density, this may not explain our findings for the reasons outlined above. It is possible that the increased amplitude in DNE cells reflects plasticity of the presynaptic release mechanism. Presynaptic release is governed by the neurotransmitter content of presynaptic vesicles (Sulzer and Edwards, 2000), differential vesicle filling and release (Rahamimoff and Fernandez, 1997; Sulzer and Pothos, 2000), the size of the pore that connects the vesicle and the plasma membrane, and how long the pore remains open after vesicle fusion. Additionally, increased intracellular Ca^{2+} in presynaptic terminals may increase synchronous release of quanta and thus increase mEPSC amplitude (Kirischuk and Grantyn, 2000; Llano et al., 2000), but whether or how DNE alters intracellular calcium kinetics is not clear. Finally, it is plausible that DNE caused a shift towards mEPSCs originating at synaptic sites where quanta are larger. Understanding the molecular mechanisms behind the DNE-mediated increase in mEPSCs will require thorough investigation, including electron microscopy to confirm structural changes at presynaptic release sites.

In conclusion, these experiments contribute to our understanding of how DNE alters the development of excitatory neurotransmission in XIIMNs. The increased AMPA-mediated quantal size in XIIMNs from DNE animals may help explain the previously reported heightened response to microinjection of AMPA or glutamate into the hypoglossal motor nucleus (Jaiswal et al., 2013), the concomitant reduction in glutamate receptor expression (Jaiswal et al., 2013) and the reduction in the size and complexity of the dendritic tree in XIIMNs of DNE animals (Powell et al., 2016). The functional significance of these observations has yet to be established but our working hypothesis is that the increased glutamate release and reduced cell size leads to hyperexcitability of XIIMNs (Jaiswal et al., 2013; Pilarski et al., 2011), and the reduction in transmitter receptor expression is a form of homeostatic plasticity that helps to restore normal excitability. Finally, it is interesting that the frequency of rhythmic motoneuron bursting was not altered by DNE, though there was a trend towards a higher frequency in XIIMNs from DNE animals (Fig. 3), as observed previously (Wollman et al., 2016), consistent with elevated excitability. It is clear that additional studies are necessary to elucidate the precise mechanisms underlying this form of DNE-induced plasticity in the neural networks that control the structure and function of XIIMNs, as well as the functional consequences of these developmental alterations.

Acknowledgments

Authors gratefully acknowledge the technical support of Seres Cross and Jesse Wealing in conducting these experiments. This work was funded by NIH grant R01 HD071302.

References

Abreu-Villaca Y, Seidler FJ, Qiao D, Tate CA, Cousins MM, Thillai I, Slotkin TA. Short-term adolescent nicotine exposure has immediate and persistent effects on cholinergic systems: critical periods, patterns of exposure, dose thresholds. Neuropsychopharmacology. 2003; 28:1935–1949. [PubMed: 12784097]

Ballanyi K, Onimaru H, Homma I. Respiratory network function in the isolated brainstem-spinal cord of newborn rats. Prog Neurobiol. 1999; 59:583–634. [PubMed: 10845755]

Berlin I, Heilbronner C, Georgieu S, Meier C, Spreux-Varoquaux O. Newborns' cord blood plasma cotinine concentrations are similar to that of their delivering smoking mothers. Drug and alcohol dependence. 2010; 107:250–252. [PubMed: 19939584]

Donato R, Nistri A. Relative contribution by GABA or glycine to Cl(−)-mediated synaptic transmission on rat hypoglossal motoneurons in vitro. J Neurophysiol. 2000; 84:2715–2724. [PubMed: 11110802]

Dwyer JB, McQuown SC, Leslie FM. The dynamic effects of nicotine on the developing brain. Pharmacology & therapeutics. 2009; 122:125–139. [PubMed: 19268688]

Eisele DW, Schwartz AR, Smith PL. Tongue neuromuscular and direct hypoglossal nerve stimulation for obstructive sleep apnea. Otolaryngologic clinics of North America. 2003; 36:501–510. [PubMed: 12956097]

Eriksson P. Developmental neurotoxicity of environmental agents in the neonate. Neurotoxicology. 1997; 18:719–726. [PubMed: 9339819]

Eriksson P, Ankarberg E, Viberg H, Fredriksson A. The developing cholinergic system as target for environmental toxicants, nicotine and polychlorinated biphenyls (PCBs): implications for neurotoxicological processes in mice. Neurotox Res. 2001; 3:37–51. [PubMed: 15111260]

Fregosi RF, Luo Z, Iizuka M. GABAA receptors mediate postnatal depression of respiratory frequency by barbiturates. Respir Physiol Neurobiol. 2004; 140:219–230. [PubMed: 15186784]

Funk GD, Greer JJ. The rhythmic, transverse medullary slice preparation in respiratory neurobiology: contributions and caveats. Respir Physiol Neurobiol. 2013; 186:236–253. [PubMed: 23357617]

Gentry CL, Lukas RJ. Regulation of nicotinic acetylcholine receptor numbers and function by chronic nicotine exposure. Curr Drug Targets CNS Neurol Disord. 2002; 1:359–385. [PubMed: 12769610]

Ginzel KH, Maritz GS, Marks DF, Neuberger M, Pauly JR, Polito JR, Schulte-Hermann R, Slotkin TA. Critical review: nicotine for the fetus, the infant and the adolescent? Journal of health psychology. 2007; 12:215–224. [PubMed: 17284486]

Hafstrom O, Milerad J, Sandberg KL, Sundell HW. Cardiorespiratory effects of nicotine exposure during development. Respir Physiol Neurobiol. 2005; 149:325–341. [PubMed: 15970470]

Huang YH, Brown AR, Costy-Bennett S, Luo Z, Fregosi RF. Influence of prenatal nicotine exposure on postnatal development of breathing pattern. Respir Physiol Neurobiol. 2004; 143:1–8. [PubMed: 15477168]

Jaiswal SJ, Pilarski JQ, Harrison CM, Fregosi RF. Developmental nicotine exposure alters AMPA neurotransmission in the hypoglossal motor nucleus and pre-botzinger complex of neonatal rats. J Neurosci. 2013; 33:2616–2625. [PubMed: 23392689]

Kezirian EJ, Boudewyns A, Eisele DW, Schwartz AR, Smith PL, Van de Heyning PH, De Backer WA. Electrical stimulation of the hypoglossal nerve in the treatment of obstructive sleep apnea. Sleep medicine reviews. 2010; 14:299–305. [PubMed: 20116305]

Kirischuk S, Grantyn R. A readily releasable pool of single inhibitory boutons in culture. Neuroreport. 2000; 11:3709–3713. [PubMed: 11117477]

Llano I, Gonzalez J, Caputo C, Lai FA, Blayney LM, Tan YP, Marty A. Presynaptic calcium stores underlie large-amplitude miniature IPSCs and spontaneous calcium transients. Nat Neurosci. 2000; 3:1256–1265. [PubMed: 11100146]

Luo Z, McMullen NT, Costy-Bennett S, Fregosi RF. Prenatal nicotine exposure alters glycinergic and GABAergic control of respiratory frequency in the neonatal rat brainstem-spinal cord preparation. Respir Physiol Neurobiol. 2007; 157:226–234. [PubMed: 17321805]

Marks MJ, Burch JB, Collins AC. Effects of chronic nicotine infusion on tolerance development and nicotinic receptors. J Pharmacol Exp Ther. 1983; 226:817–825. [PubMed: 6887012]

Marks MJ, Stitzel JA, Collins AC. Time course study of the effects of chronic nicotine infusion on drug response and brain receptors. J Pharmacol Exp Ther. 1985; 235:619–628. [PubMed: 4078726]

Muhammad A, Mychasiuk R, Nakahashi A, Hossain SR, Gibb R, Kolb B. Prenatal nicotine exposure alters neuroanatomical organization of the developing brain. Synapse. 2012; 66:950–954. [PubMed: 22837140]

Oncken C. Nicotine replacement for smoking cessation during pregnancy. N Engl J Med. 2012; 366:846–847. [PubMed: 22375978]

Pauly JR, Slotkin TA. Maternal tobacco smoking, nicotine replacement and neurobehavioural development. Acta Paediatrica. 2008; 97:1331–1337. [PubMed: 18554275]

Pilarski JQ, Fregosi RF. Prenatal nicotine exposure alters medullary nicotinic and AMPA-mediated control of respiratory frequency in vitro. Respir Physiol Neurobiol. 2009; 169:1–10. [PubMed: 19651248]

Pilarski JQ, Wakefield HE, Fuglevand AJ, Levine RB, Fregosi RF. Developmental nicotine exposure alters neurotransmission and excitability in hypoglossal motoneurons. J Neurophysiol. 2011; 105:423–433. [PubMed: 21068261]

Pilarski JQ, Wakefield HE, Fuglevand AJ, Levine RB, Fregosi RF. Increased nicotinic receptor desensitization in hypoglossal motor neurons following chronic developmental nicotine exposure. J Neurophysiol. 2012; 107:257–264. [PubMed: 22013232]

Pinheiro PS, Mulle C. Presynaptic glutamate receptors: physiological functions and mechanisms of action. Nat Rev Neurosci. 2008; 9:423–436. [PubMed: 18464791]

Powell GL, Gaddy J, Xu F, Fregosi RF, Levine RB. Developmental Nicotine Exposure disrupts dendritic arborization patterns of hypoglossal motoneurons in the neonatal rat. Developmental neurobiology. 2016

Powell GL, Levine RB, Frazier AM, Fregosi RF. Influence of developmental nicotine exposure on spike-timing precision and reliability in hypoglossal motoneurons. J Neurophysiol. 2015; 113:1862–1872. [PubMed: 25552642]

Rahamimoff R, Fernandez JM. Pre- and postfusion regulation of transmitter release. Neuron. 1997; 18:17–27. [PubMed: 9010202]

Revill AL, Vann NC, Akins VT, Kottick A, Gray PA, Del Negro CA, Funk GD. Dbx1 precursor cells are a source of inspiratory XII premotoneurons. eLife. 2015:4.

Slotkin TA. Cholinergic systems in brain development and disruption by neurotoxicants: nicotine, environmental tobacco smoke, organophosphates. Toxicol Appl Pharmacol. 2004; 198:132–151. [PubMed: 15236950]

Steenland HW, Liu H, Sood S, Liu X, Horner RL. Respiratory activation of the genioglossus muscle involves both non-NMDA and NMDA glutamate receptors at the hypoglossal motor nucleus in vivo. Neuroscience. 2006; 138:1407–1424. [PubMed: 16476523]

Sulzer D, Edwards R. Vesicles: equal in neurotransmitter concentration but not in volume. Neuron. 2000; 28:5–7. [PubMed: 11086975]

Sulzer D, Pothos EN. Regulation of quantal size by presynaptic mechanisms. Reviews in the neurosciences. 2000; 11:159–212. [PubMed: 10718152]

Vautrin J, Barker JL. Presynaptic quantal plasticity: Katz's original hypothesis revisited. Synapse. 2003; 47:184–199. [PubMed: 12494401]

Wollman LB, Haggerty J, Pilarski JQ, Levine RB, Fregosi RF. Developmental nicotine exposure alters cholinergic control of respiratory frequency in neonatal rats. Developmental neurobiology. 2016

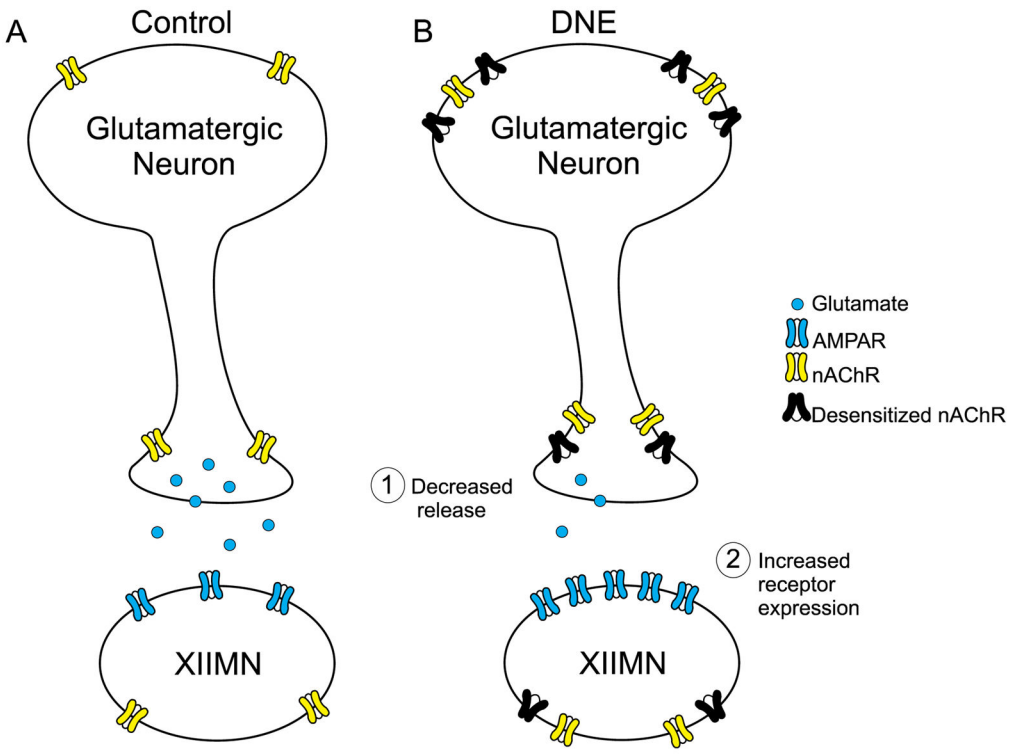

Figure 1.

Diagram illustrating possible mechanisms of DNE-induced plasticity of glutamatergic neurotransmission in XIIMNs. (A) The nAChRs on glutamatergic neurons are located on the soma, and also on the presynaptic terminals. When nicotine or ACh binds to nAChRs on the soma of the glutamatergic neuron, sufficient depolarization can evoke action-potential-dependent release of glutamate. When terminal nAChRs are stimulated by nicotine or ACh, vesicular release of glutamate is increased secondary to a rise in intracellular calcium; this reinforces the random, spontaneous vesicular release of glutamate. The XIIMNs express both nAChRs and AMPA receptors. (B) DNE is associated with an increase in nAChRs on both the cell body and terminals, but many of these receptors are in a desensitized state. As explained in the text, the net effect of DNE is a “functional loss” of nAChR-mediated synaptic transmission. This functional loss could lead to both presynaptic (decreased glutamate release) and postsynaptic (upregulation of glutamate receptor expression) plasticity.

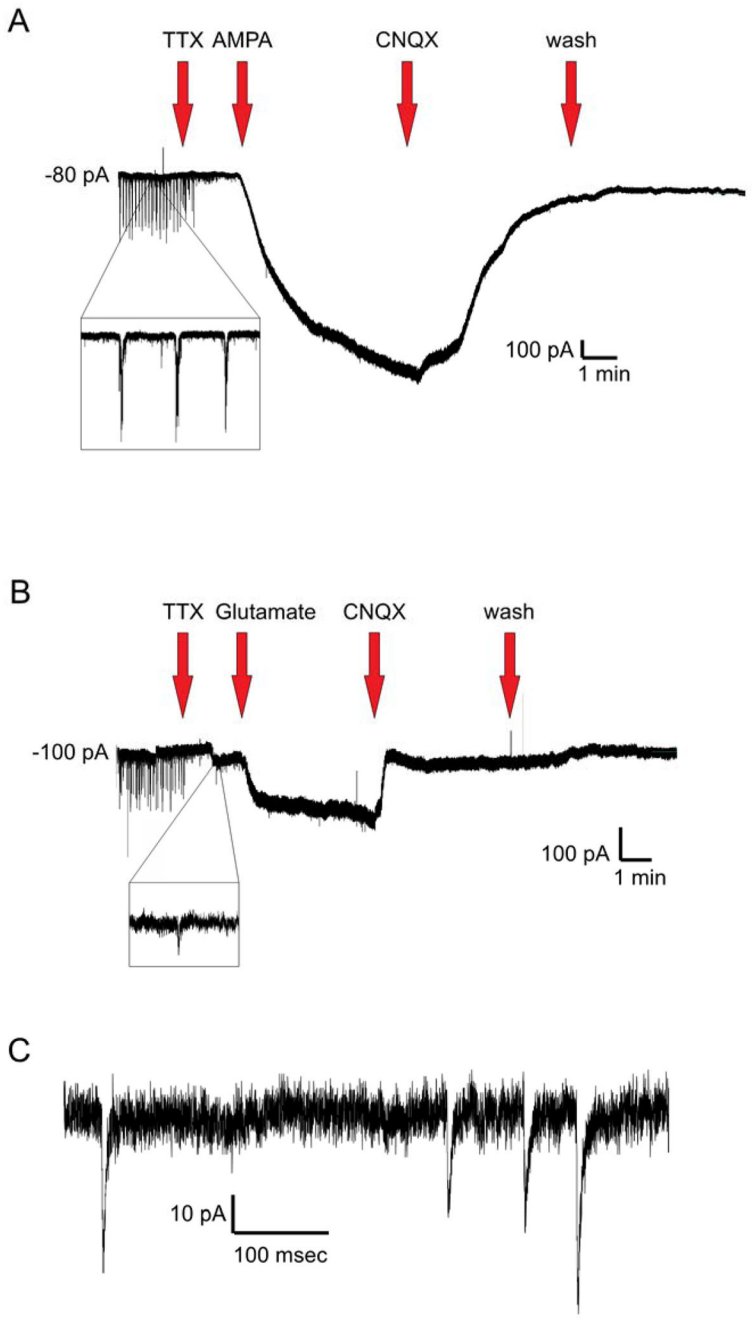

Figure 2.

(A) Representative voltage-clamp (Vhold=−70mV) recording in a rhythmically active XIIMN demonstrating the timeline of pharmacological treatments. After documenting that the XIIMNs were bursting rhythmically, TTX was applied to block action potential-dependent synaptic transmission, followed by a cocktail of AMPA and TTX, which produced a large inward current. To antagonize the effects of AMPA, a cocktail containing CNQX, AMPA, and TTX was applied, followed by washout in TTX alone. (B) Same as in A, except AMPA was replaced with glutamate in this cell. All drugs were bath-applied. A

zoomed-in view of spontaneous respiratory-related bursting is shown in A, while a close up view of mEPSCs recorded after TTX are shown in B. (C) Zoomed-in view of the mEPSCs recorded after TTX application. For concentrations and durations of drug applications, see Table 1.

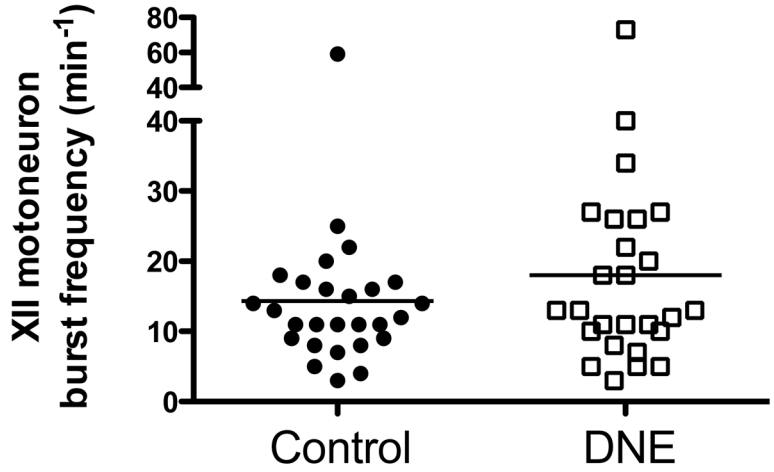

Figure 3.

Baseline rhythmic hypoglossal motoneuron burst frequency in cells from control and DNE animals. The trend towards a higher frequency in the DNE pups was not statistically significant (P = 0.2935, unpaired t-test).

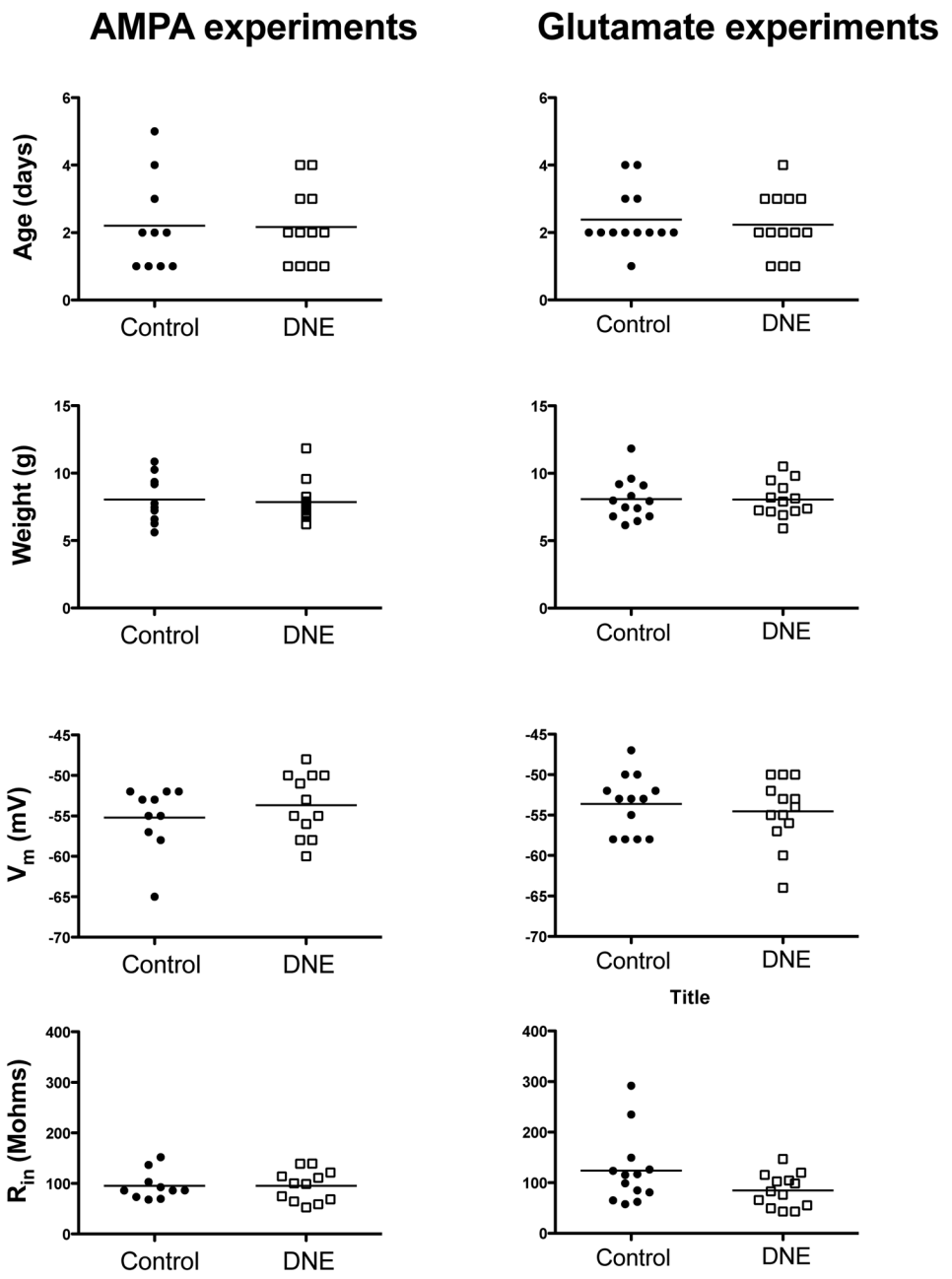

Figure 4.

Age and weight of the animals used in the AMPA and glutamate experiments (upper four panels), and the resting membrane potential (V_m) and input resistance (R_{in}) for XII motoneurons used in AMPA and glutamate experiments (lower four panels). DNE is not associated with significant differences in any of these variables.

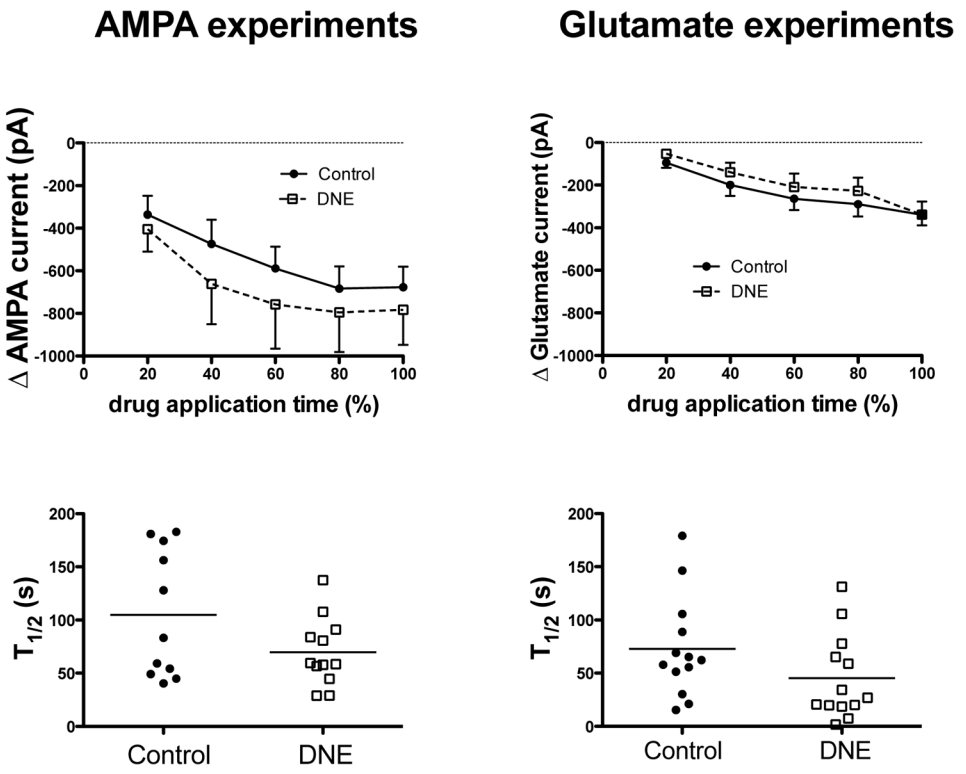

Figure 5.

Upper panels show the change in XIIMN inward current in response to bath application of 2.5 μM AMPA (left panel) or 200 μM glutamate (right panel). The change in current is expressed as a function of the total drug application time (see Fig. 2). Note that in both treatment groups, bath application of AMPA produced a greater inward current than bath application of glutamate. With both drugs, the change in inward current was significant ($P < 0.0001$, 2-way ANOVA), but there were no significant treatment effects or time-treatment interactions, suggesting a similar response in cells control and DNE animals. *Lower panels* show the time to reach half of the peak inward current ($T_{1/2}$) in each XIIMN studied in response to AMPA (left panel) or glutamate (right panel). Though there is a clear trend for a more rapid response in cells from DNE animals, the differences were not significant for either the AMPA ($P = 0.09$) or glutamate ($P = 0.12$) experiments.

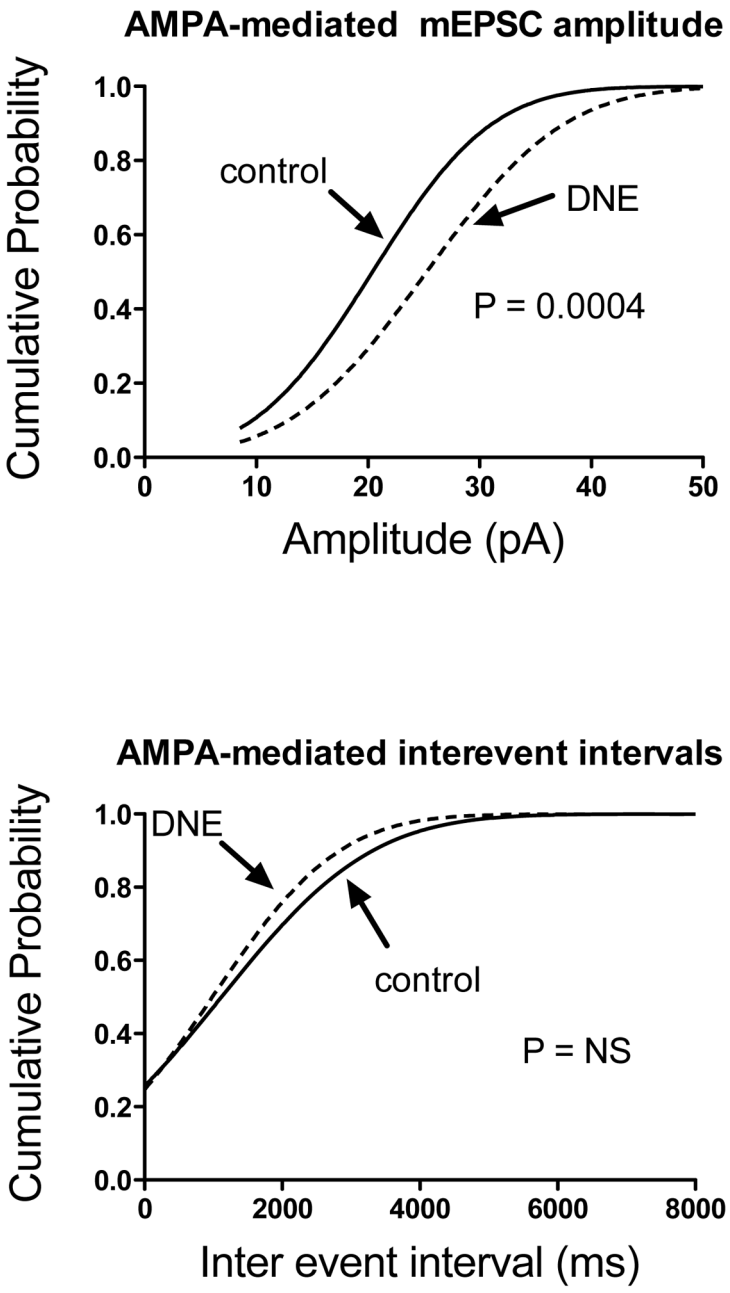

Figure 6.

Cumulative probability distribution of mEPSC amplitudes (top panel) and interevent intervals (bottom panel) recorded in the first minute of AMPA bath application in 11 control and 12 DNE cells. The probability distributions were constructed on the pooled data, using every mEPSC that was analyzed (control, 165 total mEPSCs; DNE, 150 total mEPSCs). As indicated in Results, CNQX resulted in the cessation of the mEPSCs confirming that they are glutamatergic. The amplitude distribution in cells from DNE animals was shifted to the right indicating an overall increase in the amplitude of mEPSCs, and this difference was statistically significant (P = 0.0004). The interevent interval distribution in cells from DNE

animals was shifted slightly to the left, but the probability distributions from control and DNE cells were not significantly different.

Table 1

Concentration and duration of drug application used in the experiments outlined in Figure 2. All drugs were dissolved in oxygenated (95% O_2/5% CO_2) aCSF (KCl 9mM), and were bath-applied at 27°C.

Drug(s) Applied	Concentration	Duration (min)
TTX	1 μM	2 min
AMPA/TTX	2.5 μM/1 μM	5 min
CNQX/AMPA/TTX	20 μM/2.5 μM/1 μM	5 min
Glutamate/TTX	200 μM/1 μM	5 min
CNQX/Glutamate/TTX	20 μM/200 μM/1 μM	5 min
Wash/TTX	−/1 μM	5 min